Journal of Applied Mechanics and Technical Physics, Vol. 41, No. 2, 2000

SEDIMENT-DISCHARGE VECTOR IN A TURBULENT FLOW ABOVE AN ERODED BOTTOM

A. G. Petrov and P. G. Petrov

UDC 532.545

The problem of determination of sediment discharge by a turbulent flow of a fluid above an eroded surface of an arbitrary relief with a finite slope of the bottom is considered. The surface of the bottom separates a stationary granular medium (sand) from a moving two-phase mixture of a fluid and solid particles. The medium is set into motion under the action of shear stress of the fluid. The medium obeys Coulomb's friction law for a granular medium and Prandtl's law of turbulent friction of the fluid. As a result of solving the boundary-value problem for the motion of a two-phase mixture of a fluid and solid particles, a generic formula for sediment discharges is derived. The sediment-discharge vector is expressed through the vector of shear stress on the bottom, the vector of the slope of the bottom, and the distribution function of the solid particles in the bottom layer for an arbitrary relief of the bottom with a finite slope. It is shown that the sediment discharge depends weakly on the detailed distribution of particles in the bottom layer. Conditions of failure of the bottom surface are obtained. The sediment-discharge formula allows one to derive a closed system of equations that determines the process of bottom erosion in the river or channel bed.

The theory of motion of suspended particles in a turbulent flow with a low concentration was developed by Kolmogorov [1] and Barenblatt [2]. Bagnold [3] suggested that Coulomb's dry friction between the solid particles moving in a fluid should be taken into account. In [4–8], the motion of a mixture of a fluid and solid particles is studied using a rheological relation in the form of a combination of dry friction for the solid phase and viscous friction for the fluid phase. A one-dimensional turbulent flow over a smooth bottom is studied in [4–6]. An analytical relation for the sediment-discharge vector for the bottom relief with a small slope was found for a three-dimensional turbulent flow [7, 8].

1. Geometrical Description of the Bottom Surface. We give exact formulas for local characteristics of the bottom surface not assuming the slope of the surface to be small. Let X, Y, Z be a stationary Cartesian coordinate system with the Z axis directed vertically upward. The bottom surface in this coordinate system is determined by the equation $Z = \zeta(X, Y)$, where ζ is a rather smooth function of the variables X and Y. The normal vector $\boldsymbol{n}$ to the bottom surface has the components

$$n_x = -\frac{\partial \zeta}{\partial X}\cos\gamma, \qquad n_y = -\frac{\partial \zeta}{\partial Y}\cos\gamma, \qquad n_z = \cos\gamma,$$

where γ is the angle between the normal $\boldsymbol{n}$ and the Z axis. Trigonometric functions of the angle γ have the form $\cos\gamma = 1/\sqrt{1+\tan^2\gamma}$ and $\tan\gamma = \sqrt{(\partial\zeta/\partial X)^2 + (\partial\zeta/\partial Y)^2}$.

The projection of the unit vector $\boldsymbol{k}$ directed vertically upwards onto the tangent plane to the surface $Z = \zeta$ will be called the slope vector $\boldsymbol{I}$ (Fig. 1), which can be decomposed into the vectors $\boldsymbol{k}$ and $\boldsymbol{n}$:

Institute Problems of Mechanics, Russian Academy of Sciences, Moscow 117526. Translated from Prikladnaya Mekhanika i Tekhnicheskaya Fizika, Vol. 41, No. 2, pp. 102–112, March–April, 2000. Original article submitted February 16, 1999.

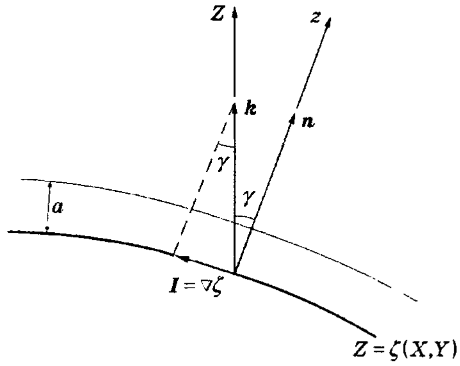

Fig. 1

$\boldsymbol{I} = \boldsymbol{k} - \boldsymbol{n} \cos\gamma$. Hence, we can easily write its components along the X, Y, and Z axes and determine its length $I = \sin\gamma$.

Along with the stationary coordinate system, we introduce a local curved orthogonal coordinate system x, y, z. The z axis is orthogonal to the surface $Z = \zeta$, and the x and y axes are the internal coordinates of this surface. In the local coordinate system, the bottom surface is described by the equation $z = 0$. The slope vector $\boldsymbol{I}$ in the local coordinate system has the components $I_x = \partial\zeta/\partial x$ and $I_y = \partial\zeta/\partial y$ or, in the vector form, $\boldsymbol{I} = \nabla\zeta$, $|\nabla\zeta| = \sin\gamma$, and $\nabla = (\partial/\partial x, \partial/\partial y)$.

2. Assumptions. We consider a turbulent flow of a heavy incompressible fluid with solid particles in the region $\zeta(X, Y) \leqslant Z \leqslant \eta(X, Y)$, where $Z = \eta$ is the free-surface equation. The region $Z \leqslant \zeta(X, Y)$ contains a stationary homogeneous granular medium through which the fluid is filtered. Mass transfer of the solid particles with density ρ_p greater than the fluid density ρ_w occurs at the interface $Z = \zeta$.

The main mass of the particles is assumed to move in the bottom layer of thickness a much less than the depth $h = \eta - \zeta$. The variation of the layer thickness a in all directions is much smaller than the variation of the bottom depth:

$$a \ll h, \qquad |\nabla a| \ll |\nabla\zeta|. \tag{2.1}$$

It is shown below that the sediment-layer thickness is estimated as hI_{mean} (I_{mean} is the mean slope of the bottom). For plain rivers and channels, the mean slope of the bottom is less than 10^{-3}; therefore, condition (2.1) is almost always satisfied.

The hydrostatic law of pressure distribution has the form $\partial p/\partial Z = -\rho g$, where $\rho = \rho_w + C(\rho_p - \rho_w)$ is the density of the mixture of solid particles and the fluid and C is the concentration of particles. Let the pressure p_a (atmospheric) be set at the fluid surface. After integration, we obtain the pressure distribution

$$p = p_a + \rho_w g(\eta - Z) + g(\rho_p - \rho_w) \int_Z^h C\, dz'.$$

With account of (2.1), we obtain the following equation for the pressure on the bottom surface with accuracy to the small quantity $a \ll h$:

$$p_\zeta = p_a + \rho_w g(\eta - \zeta). \tag{2.2}$$

The region of medium motion can be divided into three domains. In the first domain $z \leqslant 0$ (below the bottom surface), the fluid is filtered through a stationary granular medium. If there are no waves on the free surface ($\nabla\eta = 0$) and the conditions are close to hydrostatic equilibrium, the filtration rate is much smaller than the fluid velocity in the domain $z > 0$ (above the bottom surface). The estimates show that the effect of filtration is significant in the case of a rather high gradient of the free surface and large dimensions of solid particles. Below, we consider the opposite situation where the filtration rate is close to zero.

In the second domain $z > a$, the solid phase is in a suspended state and is transported by a turbulent fluid flow as a passive admixture. In accordance with the gravitational theory developed in [1, 2], the concentration of particles decreases following the power law $C = C_0(a/z)^K$, $K = W/(æU_*)$, where U_* is the dynamic velocity, W is the particle-sedimentation velocity in a quiescent fluid (settling velocity), and $æ \approx 0.4$ is the von Kármán constant. The Schields parameter is $K \approx 12$ for a flow velocity close to the starting velocity of the particles ($U_{*\rm st} \approx 0.2W$). For $K \in (3, 12)$ (the case of the greatest practical interest), the contribution of suspended particles to the sediment discharge is negligibly small as compared to the main contribution of the bottom sediment in the domain $0 \leqslant z \leqslant a$. Thus, to calculate the discharge, it is sufficient to study the mixture flow in the third domain $0 \leqslant z \leqslant a$ where the friction of particles, the turbulent transport, and the force of gravity should be taken into account.

3. Mathematical Model. We consider a mathematical model of motion of a mixture of a fluid and particles in a thin bottom layer $0 \leqslant z \leqslant a$. Acceleration of the particles of the medium moving steadily in a thin layer is negligibly small as compared to friction forces: $\rho|dv/dt| \ll |\partial\tau/\partial z|$.

Equations of Motion. The hydrodynamic law acts across the thin layer, and the equation of balance of the friction forces, pressure gradient, and gravity is fulfilled along the layer:

$$\frac{\partial \boldsymbol{\tau}}{\partial z} = \nabla p_\zeta + \rho g \nabla \zeta, \qquad \rho = \rho_p C + \rho_w (1 - C). \tag{3.1}$$

Equation (3.1) is similar to the Reynolds equation for a thin layer of a viscous fluid.

Rheological Law. The relationship between the shear stress $\boldsymbol{\tau}$ and the strain rate $\partial \boldsymbol{v}/\partial z$ can be determined by the tensor function $\boldsymbol{\tau}(\partial \boldsymbol{v}/\partial z)$ that generalizes Prandtl's law for a turbulent fluid layer and Coulomb's dry friction law for solid particles. The dependence satisfying these requirements has the form

$$\boldsymbol{\tau} = (\tau_w + \tau_p)\,\boldsymbol{e}, \qquad \boldsymbol{e} = \frac{\partial \boldsymbol{v}}{\partial z}\Big|\frac{\partial \boldsymbol{v}}{\partial z}\Big|^{-1}; \tag{3.2}$$

$$\tau_w = (æz)^2 \Big|\frac{\partial \boldsymbol{v}}{\partial z}\Big|^2 \rho_w; \tag{3.3}$$

$$\tau_p = p_p \tan\varphi, \qquad p_p = (\rho_p - \rho_w) g \cos\gamma \int_z^a C\,dz'. \tag{3.4}$$

Here τ_w and τ_p are the absolute values of the shear stress of the fluid and solid phases, $\boldsymbol{e}$ is the unit vector aligned with the vector $\partial \boldsymbol{v}/\partial z$, p_p is the pressure of solid particles suspended in water, and φ is the angle of internal friction ($\varphi \approx 30°$ for sand). Prandtl's law is described by formula (3.3) and Coulomb's dry friction law for the solid phase by formula (3.4).

The system of equations (3.1)–(3.4) supplemented by the diffusion equation was introduced in [7, 8]. For a particular case of a one-dimensional flow above a smooth bottom, these equations can be found in [4–6].

Not supplementing yet the equation determining the distribution of the concentration, we consider the latter by a known function $C(z)$. Then the general formulas for sediment discharges contain the distribution function of the particles in the layer $0 \leqslant z \leqslant a$, which is expressed via $C(z)$:

$$f(z) = \int_z^a C\,dz' \Big/ \int_0^a C\,dz'. \tag{3.5}$$

Boundary Conditions. The boundary conditions can be derived from the continuity of velocity and shear stress on the basis of the following reasoning [7, 8]. For $z \leqslant 0$, the medium is at rest: $v = 0$. The shear stress in a quiescent medium does not exceed Coulomb's friction: $\tau \leqslant p_p \tan\varphi$. In a moving medium, for $z > 0$, according to the rheological law (3.2), (3.3) accepted, we have $\tau = p_p \tan\varphi + \tau_w$, and $\tau_w \geqslant 0$. The continuity of τ at the point $z = 0$ is possible only under the condition $\tau_w = 0$. Thus, we obtain the conditions

$$z = 0: \qquad \boldsymbol{v} = 0, \quad \tau_w = 0, \quad f = 1. \tag{3.6}$$

It should be noted that the velocity distributions in the problem considered and in the problem without particles are significantly different despite an identical law of turbulent friction (3.3). For a pure fluid near the wall, we have $\tau_w \approx$ const, which leads to a logarithmic law of velocity distribution. According to (3.6), τ_w for the mixture increases proportionally to the distance from the wall, and the velocity distribution law is linear near $z = 0$.

The shear stress $\boldsymbol{T}$ is set at the upper boundary of the wall. The solid particles pass to a suspended state, and we have $\tau_p = 0$. Hence, we obtain the boundary conditions

$$z = a: \qquad \boldsymbol{\tau} = \boldsymbol{T}, \quad \tau_p = 0, \quad f = 0. \tag{3.7}$$

By virtue of conditions (2.1), we can ignore the layer thickness a and consider the value of $\boldsymbol{T}$ to be equal to that in a pure fluid on the bottom $Z = \zeta$; therefore, $\boldsymbol{T}$ is calculated from the solution of the hydrodynamic problem (in the absence of solid particles).

4. Derivation of the Sediment-Discharge Formula. We pass from the variable z to a new variable f (3.5). If there are no waves on the free surface ($\nabla\eta = 0$), the pressure gradient in the bottom layer is $\nabla p_\zeta = -\rho_w g \nabla\zeta$ in accordance with (2.2). Then Eqs. (3.1) and (3.4) are written as

$$\frac{\partial \boldsymbol{\tau}}{\partial f} = -T a_1 \boldsymbol{\Gamma}, \qquad \frac{\partial \tau_p}{\partial f} = T a_1, \qquad df = -C\,dz \Big/ \int\limits_0^a f\,dz; \tag{4.1}$$

$$\boldsymbol{\Gamma} = \frac{\nabla\zeta}{\cos\gamma \tan\varphi}, \qquad |\boldsymbol{\Gamma}| = \frac{\tan\gamma}{\tan\varphi}; \tag{4.2}$$

$$a_1 = \frac{(\rho_p - \rho_w) g \tan\varphi \cos\gamma}{T} \int\limits_0^a C\,dz. \tag{4.3}$$

Integrating Eq. (4.1) with account of condition (3.7), we can find the following relations for the total stress vector τ and for the stresses in the solid and fluid phases:

$$\boldsymbol{\tau} = T\boldsymbol{F}, \qquad \tau_p = T a_1 f, \qquad \tau_w = |\tau| - \tau_p = T(F - a_1 f); \tag{4.4}$$

$$\boldsymbol{F} = \boldsymbol{s} - \boldsymbol{\Gamma} a_1 f(z), \qquad F = |\boldsymbol{F}| = \sqrt{(1 - \Gamma_x a_1 f)^2 + (\Gamma_y a_1 f)^2}. \tag{4.5}$$

Here $\boldsymbol{s}$ is the unit vector collinear to the vector $\boldsymbol{T}$ and the x axis is aligned with the vector $\boldsymbol{s}$.

The constant a_1 can be expressed in terms of Γ_x and Γ_y. For this purpose, we use conditions (3.6) at the bottom. It follows from (4.4) that $\tau_W = 0$, $f = 1$, and $F = a_1$ for $z = 0$. Substituting these values into (4.5), we obtain the following equation for a_1:

$$(1 - \Gamma_x a_1)^2 + (\Gamma_y a_1)^2 = a_1^2 \;\Rightarrow\; (1/a_1 - \Gamma_x)^2 = 1 - \Gamma_y^2. \tag{4.6}$$

The existence of a positive root of Eq. (4.6) determines the range of variation of the slope vector $\boldsymbol{\Gamma}$. In Fig. 2, this region is shown in the plane Γ_x, Γ_y. The only positive root exists inside the circle of unit radius $|\boldsymbol{\Gamma}| < 1$, on some part of the arc of this circle we have $|\boldsymbol{\Gamma}| = 1$ and $\Gamma_x > 0$, and also on the rays $\Gamma_y = \pm 1$ and $\Gamma_x > 0$. This root is equal to

$$a_1 = \frac{1}{\Gamma_x + \sqrt{1 - \Gamma_y^2}}. \tag{4.7}$$

Two positive roots exist in the right half-band bounded by the arc of the circle $|\Gamma_y| < 1$, $|\boldsymbol{\Gamma}| > 1$: $a_1 = 1/(\Gamma_x \pm \sqrt{1 - \Gamma_y^2})$.

The bifurcation of the solution (branching of the second root) occurs at the points $\Gamma_y \pm 1$. The existence of the second root depends on its stability. If the bottom surface satisfies the condition $|\tan\gamma| < \tan\varphi$ at the initial time and we have $|\Gamma_y| < 1$ afterwards, the second root is absent. This follows from the continuity

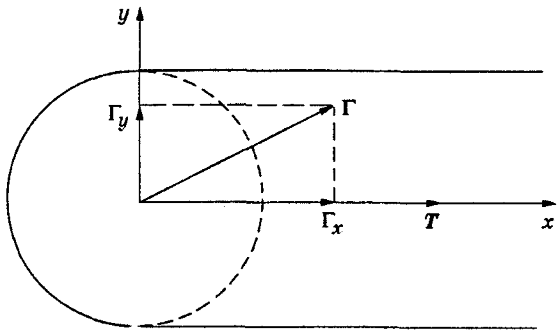

Fig. 2

of the dependence of a_1 on the vector $\mathbf{\Gamma}$. In what follows, we confine ourselves to studying the first branch of the root (4.7).

Equalities (4.5) and (4.7) determine the dependence $F(f)$ for a given vector $\mathbf{\Gamma}(\Gamma_x, \Gamma_y)$, which has the following expansions for $f = 0$ and $f = 1$:

$$F \approx 1 - \Gamma_x a_1 f, \quad f \ll 1, \qquad F \approx a_1 f + \sqrt{1 - \Gamma_y^2}(1 - f), \quad 1 - f \ll 1.$$

Thus, the function $F(f)$ increases monotonically within the interval $f \in (0, 1)$ from $F(0) = 1$ to $F(1) = a_1$. The distributions of the characteristics in the layer are exactly expressed through the functions F and $F - a_1 f$, which depend on the argument f, and the unit vector $\mathbf{e}$ of the form

$$\mathbf{e} = (\mathbf{s} - \mathbf{\Gamma} a_1 f(z))F^{-1}, \qquad e_x = (1 - \Gamma_x a_1 f)F^{-1}, \quad e_y = -\Gamma_y a_1 f F^{-1}. \tag{4.8}$$

In what follows, we also use expansions with accuracy to the third powers of Γ_x and Γ_y:

$$F^{-1} \approx 1 + f\Gamma_x - f(1 - f)\Gamma_x^2 - f^2\Gamma_y^2/2, \quad F - a_1 f \approx (1 - f)(1 - f\Gamma_y^2/2),$$
$$e_x \approx 1 - f^2\Gamma_y^2/2, \qquad e_y \approx -f\Gamma_y[1 - (1 - f)\Gamma_x]. \tag{4.9}$$

We now find the velocity distribution of the mixture and the sediment discharge. From (3.3) and (4.4), we have

$$\left|\frac{\partial \mathbf{v}}{\partial z}\right| = U_* \frac{\sqrt{F - a_1 f}}{æ z}, \qquad \frac{\partial \mathbf{v}}{\partial z} = \mathbf{e}\left|\frac{\partial \mathbf{v}}{\partial z}\right|. \tag{4.10}$$

From (3.5) and (4.3), we obtain

$$\Phi_0 = \int_0^a C\, dz = \frac{T a_1}{(\rho_p - \rho_w) g \tan\varphi \cos\gamma}, \qquad C\, dz = -\Phi_0\, df. \tag{4.11}$$

Using (4.11), the sediment discharge $\mathbf{G}$ can be represented in the form

$$\mathbf{G} = \rho_p \int_0^a C\mathbf{v}\, dz = -\rho_p \Phi_0 \int_0^a \mathbf{v}(z)\, df. \tag{4.12}$$

Integrating by parts, we find

$$-\int_0^a \mathbf{v}\, df(z) = -\mathbf{v} f\Big|_0^a + \int_0^a f \frac{\partial \mathbf{v}}{\partial z}\, dz. \tag{4.13}$$

The first term in the right part is equal to zero by virtue of the conditions $\mathbf{v}(0) = 0$ and $f(a) = 0$. Substituting relations (4.10) into (4.13), we obtain

$$-\int_0^a \mathbf{v}\, df(z) = \frac{U_*}{æ} \int_0^a \frac{f\sqrt{F - a_1 f}}{z}\, \mathbf{e}\, dz. \tag{4.14}$$

The exact value of integral (4.14) is represented in the form of decomposition into the vectors $\boldsymbol{s}$ and $\boldsymbol{\Gamma}$:

$$-\int_0^a \boldsymbol{v}\, df(z) = \frac{U_*}{æ} [(A + B\Gamma_x)\, \boldsymbol{s} - B\boldsymbol{\Gamma}],$$

$$A = \int_0^a \frac{f\sqrt{F - a_1 f}}{z} e_x\, dz, \qquad -B\Gamma_y = \int_0^a \frac{f\sqrt{F - a_1 f}}{z} e_y\, dz. \tag{4.15}$$

Substituting (4.15) into (4.12), we obtain the sediment-discharge formula

$$\boldsymbol{G} = G_0 a_1 [(A + B\Gamma_x)(\boldsymbol{T}/|\boldsymbol{T}|) - B\boldsymbol{\Gamma}], \tag{4.16}$$

where

$$G_0 = \rho_p \Phi_0 \frac{U_*}{æ a_1} = \frac{\rho_p U_*^3}{æ g \tan\varphi \cos\gamma} \frac{\rho_w}{\rho_p - \rho_w}, \quad U_* = \sqrt{\frac{T}{\rho_w}}.$$

Relation (4.16) can be used for finite values of the slope vector. The factor a_1 determined from (4.7) turns to infinity at $|\boldsymbol{\Gamma}| = 1$ and $\Gamma_x \leqslant 0$. This condition defines the critical slope at which the failure occurs.

We obtain expansions for the coefficients A and B with accuracy to the third powers of Γ_x and Γ_y by substituting expansions (4.9) into (4.15). Confining ourselves to linear and quadratic terms in this equality, we obtain

$$A \approx A_0 + A_2 \Gamma_y^2, \qquad B \approx B_0 + B_1 \Gamma_x; \tag{4.17}$$

$$A_0 = \int_0^1 \frac{f\sqrt{1-f}}{z}\, dz, \qquad A_2 = -\int_0^1 \frac{f^2(1/2 + f)\sqrt{1-f}}{2z}\, dz,$$

$$B_0 = \int_0^1 \frac{f^2\sqrt{1-f}}{z}\, dz, \qquad B_1 = -\int_0^1 \frac{f^2(1-f)^{3/2}}{z}\, dz. \tag{4.18}$$

5. Analysis of the Discharge Formula. The coefficients in (4.17) determining the discharge vector depend on the form of the function $f(z)$. However, according to definition (3.5), the function $f(z)$ satisfies the restrictions

$$0 \leqslant f \leqslant 1, \quad f(0) = 1, \quad f(a) = 0, \quad f'_z = -C/\Phi_0 < 0, \quad f''_z = -C'_z/\Phi_0 \geqslant 0. \tag{5.1}$$

We can show that the coefficients in formulas (4.18) change insignificantly under these restrictions on f. Indeed, we consider the functions of the form $f = (1 - z/a)^\beta$. We can easily see that these functions satisfy restrictions (5.1) for $\beta \geqslant 1$. For $\beta = 1$, the integrals in (4.18) acquire the following values:

$$A_0 = 4/3, \qquad A_2 = -76/105, \qquad B_0 = 16/15, \qquad B_1 = -16/105. \tag{5.2}$$

Within the interval $\beta \in (1, 3)$, the coefficients of (5.2) change by less than 10%, which is seen from Fig. 3. In [8], the distribution function is found from the solution of the turbulent diffusion equation, and the calculated coefficients are also little different from the values of (5.2).

Thus, we assume that the parameter β equals unity and the function f is linear ($f = 1 - z/a$). From formulas (4.3), (4.5), (4.8), and (4.15), we can determine exactly the coefficients A and B in the discharge formula. We denote the deviations of the exact values of A and B from their approximate values (4.17) and (5.2) as ΔA and ΔB. For a fixed value of Γ_y, the greatest values of $|\Delta A|$ and $|\Delta B|$ are reached for $\Gamma_x \approx 0$. The greatest values of ΔA and ΔB versus Γ_y for $\Gamma_x = 0$ are listed in Table 1.

Thus, the vector dependence (4.16) with coefficients (4.17) and (5.2) determines the discharge vector $\boldsymbol{G}$ rather accurately for all values of the vector $\boldsymbol{\Gamma}$ within the region shown in Fig. 2. If the x axis is aligned with

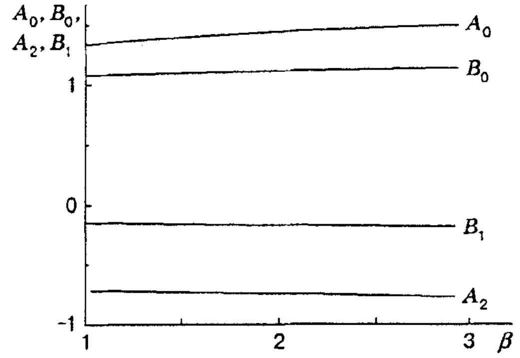

Fig. 3

TABLE 1

Γ_y	ΔA	ΔB
0.2	−0.0007	−0.0042
0.4	−0.0013	−0.0185
0.6	−0.0221	−0.0499
0.8	−0.1070	−0.1252

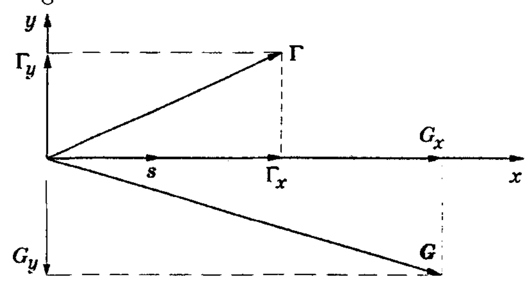

Fig. 4

the vector $\boldsymbol{T}$, then the vector $\boldsymbol{G}$ has the components $G_x = G_0 a_1 A$ and $G_y = -G_0 a_1 B \Gamma_y$ (Fig. 4). Depending on the value of $\boldsymbol{\Gamma}$, the factor a_1 takes any positive values up to infinity for the critical values $\Gamma_x = -\sqrt{1-\Gamma_y^2}$.

6. Comparison with Experiment. In calculating the erosion process, the balance equation for the solid particles on the bottom surface is usually used:

$$\frac{\partial(\zeta\cos\gamma)}{\partial t} + \frac{1}{\rho_p(1-\varepsilon)}\Big(\frac{\partial G_x}{\partial x} + \frac{\partial G_y}{\partial y}\Big) = 0. \tag{6.1}$$

The discharge vector is usually calculated using an empirical formula based on one-dimensional flow measurements on a smooth bottom (Meyer-Peter and Miller's formula is most frequently used [9]). The direction of $\boldsymbol{G}$ coincides with the flow velocity. Using such a method of calculation, it is impossible to explain the erosion process in a constant-section channel with a slope (the slope vector is directed perpendicular to the channel axis). Indeed, if the x axis is directed along the channel centerline, the vector $\boldsymbol{G}$ has only one component G_x, which is independent of x. From (6.1), we obtain $\partial\zeta/\partial t = 0$. Conversely, in accordance with formula (4.16), the vector $\boldsymbol{G}$ has (apart from G_x) the component $G_y = -G_0 B \cot\varphi(\partial\zeta/\partial y)$, which determines the erosion process at the slope. The factor G_0 is calculated by formula (4.16), and the dynamic velocity is expressed in terms of the bottom slope along the channel centerline $U_* = \sqrt{ghI}$. Figure 5 shows the channel cross section: the bottom surface at the initial time (dashed curves), the free surface (dotted curves), the theoretical dependences found by solving Eq. (6.1) (solid curves), and the experimental values of the bottom depth measured after 0.7 and 1.1 h (crosses). The water discharge is $Q = 0.187$ m^3/sec. A similar comparison for different values of the discharge also demonstrates good agreement between the theory and the experiment [7].[1]

7. Effect of the Relative Velocity of Particles. It was assumed in the model that the solid particles and the fluid have identical velocities (one-velocity model). Therefore, the resultant discharge formula (4.16) does not determine the experimentally known value of the starting velocity of the particles (the least value of the dynamic velocity at which the motion of particles in the bottom layer begins).

[1]The experiments were conducted by A. N. Militeev and N. L. Moizhes at the Hydraulic Laboratory of the Institute of Transport Construction (Moscow).

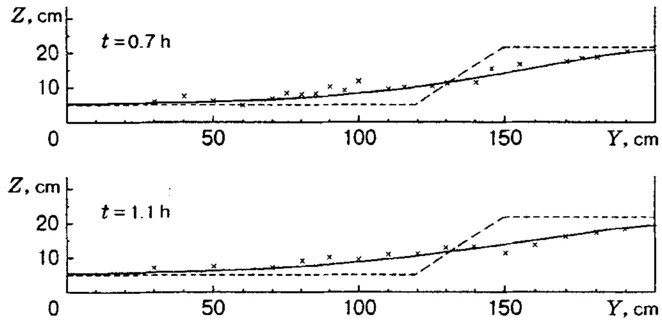

Fig. 5

Following [8], the effect of the relative velocity can be taken into account in considering the balance of forces acting on a unit volume of solid particles. The acceleration of particles in a thin layer $0 \leqslant z \leqslant a$ may be ignored:

$$\boldsymbol{F}_w + \boldsymbol{F}_p + \boldsymbol{F}_g = 0. \tag{7.1}$$

Here $\boldsymbol{F}_w$ is the drag force acting on the particles from the side of water, $\boldsymbol{F}_p$ is the friction force between the particles, and $\boldsymbol{F}_g$ is the force of gravity.

For particles of diameter greater than 0.2 mm, the drag force is proportional to the squared relative velocity of the particles $\boldsymbol{v}_r$. The drag coefficient can be found from the condition of equality of the forces of gravity and drag for an incident heavy particle

$$\boldsymbol{F}_w = -(\rho_p - \rho_w) g C \frac{\boldsymbol{v}_r |\boldsymbol{v}_r|}{W^2}, \tag{7.2}$$

where W is the sedimentation velocity of the heavy particle in the fluid.

The friction force between the particles is determined from rheological relation (3.4) for the solid-phase stress:

$$\boldsymbol{F}_p = \frac{\partial(\tau_p \boldsymbol{e})}{\partial z} = -(\rho_p - \rho_w) g C \frac{\partial(\boldsymbol{e} f)}{\partial f} \tan\varphi \cos\gamma. \tag{7.3}$$

The projection of the force of gravity onto the tangent plane to the bottom surface is represented as

$$\boldsymbol{F}_p = -(\rho_p - \rho_w) g C \boldsymbol{\Gamma} \tan\varphi \cos\gamma. \tag{7.4}$$

From (7.1)–(7.4), we obtain the following relation for the relative velocity of the particles:

$$\frac{\boldsymbol{v}_r |\boldsymbol{v}_r|}{W^2} = -\frac{\boldsymbol{e}_1}{a_1} \tan\varphi \cos\gamma, \qquad \boldsymbol{e}_1 = a_1 \Big[\boldsymbol{\Gamma} + \frac{\partial(\boldsymbol{e} f)}{\partial f}\Big]. \tag{7.5}$$

If the relative velocity is taken into account, the discharge $\boldsymbol{G}$ changes by

$$\Delta\boldsymbol{G} = \rho_p \int_0^a C \boldsymbol{v}_r \, dz = -\rho_p \Phi_0 \int_0^a \boldsymbol{v}_r \, df(z), \tag{7.6}$$

where $\boldsymbol{v}_r$ is found from (7.5):

$$\boldsymbol{v}_r = -W \sqrt{\frac{\tan\varphi \cos\gamma}{a_1}} \, \frac{\boldsymbol{e}_1}{\sqrt{|\boldsymbol{e}_1|}}.$$

Substituting this relation into (7.6), we obtain

$$\Delta\boldsymbol{G} = \boldsymbol{J} \rho_p \Phi_0 W \sqrt{\frac{\tan\varphi \cos\gamma}{a_1}}, \qquad \boldsymbol{J} = \int_0^1 \frac{\boldsymbol{e}_1}{\sqrt{|\boldsymbol{e}_1|}} \, df. \tag{7.7}$$

The vector $\boldsymbol{J}$ is independent of the particle-distribution function in the layer $f(z)$. It can be calculated by decomposing the integrand function with accuracy to terms of order Γ^3:

TABLE 2

Γ_y	ΔJ_x	ΔJ_y
0.2	0	−0.0010
0.4	−0.0008	−0.0085
0.6	−0.0055	−0.0314
0.8	−0.0302	−0.0914

$$\frac{e_{1x}}{\sqrt{|\boldsymbol{e}_1|}} = 1 + f\Big(1 - \frac{7}{4}f\Big)\Gamma_y^2, \quad \frac{e_{1y}}{\sqrt{|\boldsymbol{e}_1|}} = (1-2f)\Gamma_y - (1-f)(1-3f)\Gamma_x\Gamma_y. \tag{7.8}$$

Substituting (7.8) into (7.7), we obtain expansions for the vectors $\boldsymbol{J}$ and $\Delta\boldsymbol{G}$ with accuracy to third-order terms in Γ_x and Γ_y:

$$\boldsymbol{J} \approx (1 - \Gamma_y^2/12)\boldsymbol{s}. \tag{7.9}$$

The exact value of integral (7.6) is almost identical to its approximate value (7.9), which can be seen from the results listed in Table 2 ($\Gamma_x = 0$). Here ΔJ_x and $\Delta J_y = J_y$ are the differences between the exact and approximate values of the components of the vector $\boldsymbol{J}$. As Γ_x increases, the error rapidly decreases.

Using formulas (4.16), (4.17), (5.2), (7.7), and (7.9), we can find the discharge-vector components $\boldsymbol{G} + \Delta\boldsymbol{G}$ for finite values of the slope vector $\boldsymbol{\Gamma}$:

$$G_x + \Delta G_x = G_0 a_1 A(1 - U_{*\mathrm{st}}/U_*), \qquad G_y + \Delta G_y = -G_0 a_1 B\Gamma_y,$$
$$U_{*\mathrm{st}} = æW\sqrt{\frac{\tan\varphi\cos\gamma}{a_1}}\,\frac{J}{A}, \qquad J \approx 1 - \frac{\Gamma_y^2}{12}. \tag{7.10}$$

The quantity $U_{*\mathrm{st}}$ is the starting velocity of the particles. There is no discharge in the direction of the vector $\boldsymbol{T}$ if $U_{*\mathrm{st}} \leqslant U_*$. The relation $J/A \approx (3/4)(1 + 0.5\Gamma_y^2) \approx 3/4$ depends weakly on the slope vector. From here, substituting $æ \approx 0.4$, $A = 4/3$, and $\sqrt{\tan\varphi\cos\gamma} \approx 0.7$ into (7.10), we obtain an approximate formula convenient for engineering calculations:

$$U_{*\mathrm{st}} = 0.2W/\sqrt{a_1}. \tag{7.11}$$

The dependence of the starting velocity of the particles on the bottom slope is taken into account in (7.11) by the factor a_1.

Physical Meaning of the Starting Velocity of the Particles. The formula for the starting velocity of the particles can be derived from the condition for the critical thickness of the layer. If the layer thickness a is smaller than the particle diameter d, the solid particles do not move in the layer. In this case, Coulomb's friction force between the particles is greater than the external force $\boldsymbol{T}$ applied from outside, and the motion cannot be described by the methods of mechanics of continuous media (3.1)–(3.4). We write the starting condition for particles $a > d$ taking into account equality (4.3):

$$a \approx a_1 U_*^2/((s-1)g\bar{C}\tan\varphi\cos\gamma) > d, \qquad s = \rho_p/\rho_w. \tag{7.12}$$

Here $\bar{C}$ is the mean concentration of particles in the layer. Using the formula for the sedimentation velocity of the particles $W^2 = (s-1)gd$ [9] (balance of the forces of drag and gravity), condition (7.12) can be represented in the form

$$U_*^2 > U_{*\mathrm{st}}^2, \qquad U_{*\mathrm{st}} = W\sqrt{\bar{C}\tan\varphi\cos\gamma}/\sqrt{a_1}. \tag{7.13}$$

Formula (7.13) coincides with (7.10) and (7.11) for $\bar{C} = (Jæ/A)^2 \approx 0.09$.

8. Comparison of the Formulas for the Discharge and Starting Velocity of the Particles with Empirical Dependences. One of the best fitting empirical formulas of the discharge is given by Grishanin [9]:

$$G = (8\rho_p/(s-1))\sqrt{g}(U_*^2/g - 0.047\,d)^{3/2}. \tag{8.1}$$

Using the formula for the sedimentation velocity $W^2 = (s-1)gd$ [9] and formula (7.10) for the starting velocity, we can transform Eq. (8.1) to

$$G = 8\rho_p U_*^3/((s-1)g)(1-(U_{*\mathrm{st}}/U_*)^2)^{3/2}.$$

The range $U_{*\mathrm{st}}/U_* < 0.9$ is of practical interest, wherein the discharges calculated by formulas (8.1) and (7.10) differ by no more than 20% for $\mathbf{\Gamma} = 0$.

We consider the formula for the starting velocity (7.11) for the most important cases.

Uniform Flow above a Horizontal Bottom ($\mathbf{\Gamma} = 0$). From (4.7) and (7.11), we obtain the known empirical dependence [9]

$$a_1 = 1, \qquad U_{*\mathrm{st0}} = 0.2W.$$

Flow in a Channel with a Slope. The slope of the bottom and the vector $\mathbf{\Gamma}$ are perpendicular to the channel axis x and the shear stress on the bottom. From (4.7) and (7.11), we obtain

$$\Gamma_x = 0, \qquad a_1 = 1\Big/\sqrt{1-\Gamma_y^2}, \qquad U_{*\mathrm{st}} = U_{*\mathrm{st0}}(1-\Gamma_y^2)^{1/4}.$$

This formula was derived and experimentally verified by Lane and Carlson [10].

Flow with a Large Slope Parallel to the Channel Axis. The slope of the bottom and the vector $\mathbf{\Gamma}$ are parallel to the velocity and stress $\boldsymbol{T}$. From (4.7) and (7.11), we obtain

$$\Gamma_y = 0, \quad \Gamma_x = -\tan\gamma/\tan\varphi, \quad a_1 = 1/(1+\Gamma_x), \quad U_{*\mathrm{st}} = U_{*\mathrm{st0}}\sqrt{1+\Gamma_x}.$$

The results calculated using this formula are in good agreement with the experimental data [11] for $U_{*\mathrm{st}}$ for the angles $\gamma = 0$, 12, 18, and 22°.

Conclusions. The final result for the discharge vector has not a single empirical parameter and can be used for the bottom surface with an arbitrary finite slope up to its failure. For a one-dimensional flow above a horizontal bottom, the main result coincides with the known empirical formulas [9].

The sediment-discharge formula derived leads to the condition of the beginning of the bottom-erosion process (starting of the particles), which generalizes the known cases: the Schields condition [9] for a horizontal bottom, the starting condition for the particles in a channel with a transverse slope of the bottom [10], and the experiments for a large slope of the bottom along the channel axis [11].

The principal difference of the resultant theoretical formula from the known empirical formulas is that the sediment-discharge vector contains a transverse component to the flow direction, which is proportional to the transverse component of the bottom-slope vector, whereas the empirical dependences take into account only the longitudinal component of the vector. The erosion process in channels with a bottom slope across the channel axis cannot be described by the known empirical functions, which ignore the transverse component of the sediment-discharge vector; using the sediment-discharge formula with account of the transverse component, complete agreement of the theory and experiments on bottom erosion in such channels is obtained.

REFERENCES

1. A. N. Kolmogorov, "New variant of M. A. Velikanov's gravitational theory of the motion of suspended sediments," *Vestn. Mosk. Univ., Ser. Fiz.-Mat. Estestv. Nauk*, No. 3, 41–45 (1954).
2. G. I. Barenblatt, "Motion of suspended particles in a turbulent flow in a half-space or a flat open channel of finite depth," *Prikl. Mat. Mekh.*, **19**, No. 1, 61–88 (1955).
3. R. A. Bagnold, "The flow of cohesionless grains in fluids," *Philos. Trans. Roy. Soc. London, Ser. A*, **249**, 235–297 (1956).
4. N. Kobayashi, "Fluid and sediment interaction over a plane bed," *J. Hydraul. Eng.*, **111**, No. 6 (1985).
5. K. C. Wilson, "Analysis of bed-load motion at high shear stress," *J. Hydraul. Eng.*, **113**, No. 1, 97–103 (1985).

6. F. N. Nnadi and K. C. Wilson, "Motion of contact-load at high shear stress," *J. Hydraul. Eng.*, **118**, No. 12, 1670–1684 (1992).
7. P. G. Petrov, "Motion of a granular medium in the bottom layer of a fluid flow," *Prikl. Mekh. Tekh. Fiz.*, **32**, No. 5, 72–76 (1991).
8. A. G. Petrov and P. G. Petrov, "Transfer of suspended particles above an eroded bottom by a turbulent flow," *Prikl. Mekh. Tekh. Fiz.*, **33**, No. 4, 61–69 (1992).
9. K. V. Grishanin, *Dynamics of Channel Flows* [in Russian], Gidrometeoizdat, Leningrad (1979).
10. E. W. Lane and E. J. Carlson, "Some factors affecting the stability of channels constructed in coarse granular material," in: *Proc. of the Minnesota Int. Hydraul. Convention* (1953).
11. L. R. Fernandez and R. van Beek, "Erosion and transport of bed-load sediment," *J. Hydraul. Res.*, **14**, No. 2, 127–144 (1976).